Inorg. Chem. **2009**, *48*, 325−330

Syntheses and Structures of Alkaline Earth−Transition Metal Bimetallic Complexes As Heterogeneous Hydrodechlorination Catalyst Precursors

Errun Ding,[†] Matthew R. Sturgeon,[†] Aaron Rath,[†] Xuenian Chen,[†] Mark A. Keane,[‡] and Sheldon G. Shore*,[†]

Department of Chemistry, The Ohio State University, Columbus, Ohio 43210, and Chemical Engineering, Heriot-Watt University, Edinburgh EH14 4AS, U.K.

Received October 7, 2008

A series of alkaline earth−transition metal heterobimetallic complexes $\{(DMF)_xM(\mu\text{-}CN)_yM^*(CN)_{4-y}\}_\infty$ [M = Ba: M* = Ni **1**, M* = Pd **2**, M* = Pt **3**; M = Sr: M* = Ni **4**, M* = Pd **5**, M* = Pt **6**; $x = 3$ or 4; $y = 3$ or 4] was prepared. Single-crystal X-ray diffraction analysis revealed that $\{(DMF)_4Ba(\mu\text{-}CN)_3Ni(CN)\}_\infty$ **1**, $\{(DMF)_4Sr(\mu\text{-}CN)_3Ni(CN)\}_\infty$ **4**, $\{(DMF)_4Sr(\mu\text{-}CN)_3Pd(CN)\}_\infty$ **5**, and $\{(DMF)_4Sr(\mu\text{-}CN)_3Pt(CN)\}_\infty$ **6** form isostructural one-dimensional "ladder" arrays through isocyanide linkages (M-NC-M*), while $\{(DMF)_3Ba(\mu\text{-}CN)_4Pd\}_\infty$ **2**, and $\{(DMF)_3Ba(\mu\text{-}CN)_4Pt\}_\infty$ **3** are two-dimensional puckered sheet like arrays. These bimetallic complexes can serve as effective precursors for the synthesis of supported bimetallic catalysts. It has been established that Ba−Pd/SiO_2 and Sr−Pd/SiO_2 catalysts, prepared from **2** and **5** loaded onto a silica support, delivered specific reaction rates in the hydrodechlorination of mono- and dichloro benzene that were over an order of magnitude greater than that achieved with conventional Pd/SiO_2.

Introduction

Heterometallic complexes have attracted much attention owing to their wide application as materials with novel catalytic, magnetic, electronic, and optical properties.[1] Bimetallic catalysts are used to promote a range of processes in the fine chemical and petrochemical industries.[2] The challenges associated with the preparation of bimetallic catalysts include control over metal dispersion and achievement of well-defined metal composition.[3] Supported bimetallic catalysts are typically prepared via the stepwise introduction of each metal to the support or the incorporation of both metals from solutions of the metal precursors. Bimetallic precursors offer the possibility of a simultaneous incorporation of both metals with the prospect of a synergistic effect for the two metal components that can have significant impact in many catalytic tranformations.[4] Recently, bimetallic precursors grafted onto solid surfaces have attracted much attention, where these materials exhibited enhanced catalytic performance in hydrogenation,[5] hydrodechlorination,[6] hydroformylation,[7] and NO reduction[8] reactions when compared with monometallic catalysts. The presence of the second component can induce significant changes in both activity and selectivity for many catalytic reactions because of the electronic interaction between the two metals.

We have been concerned with the syntheses of bimetallic complexes containing a noble metal catalyst (palladium) and a rare earth catalyst promoter that could be converted to catalytic nanoparticles on a support surface by reduction of

* To whom correspondence should be addressed. E-mail: shore.1@osu.edu.
† The Ohio State University.
‡ Heriot-Watt University.

(1) (a) Eddaoudi, M.; Moler, D. B.; Li, H.; Chen, B.; Reineke, T. M.; O'Keeffe, M.; Yaghi, O. M. *Acc. Chem. Res.* **2001**, *34*, 319–330. (b) Moulton, B.; Zaworotko, M. J. *Chem. Rev.* **2001**, *101*, 1629–1658. (c) Robson, R. *J. Chem. Soc., Dalton Trans.* **2000**, 3735–3744. (d) Tulsky, E. G.; Long, J. R. *Chem. Mater.* **2001**, *13*, 1149–1166.

(2) (a) Nieminen, V.; Karhu, H.; Kumar, N.; Heinmaa, I.; Ek, P.; Samoson, A.; Salmi, T.; Murzin, D. Y. *Phys. Chem. Chem. Phys.* **2004**, *6*, 4062. (b) Tian, Z.; Xu, Y.; Lin, L. *Chem. Eng. Sci.* **2004**, *59*, 1745. (c) Ramirez-Corredores, M. M.; Romero, T.; Djaouadi, D.; Hernandez, Z.; Guerra, J. *Ind. Eng. Chem. Res.* **2002**, *41*, 5385. (d) Choi, J.; Petit-Clair, C.; Uzio, D. *Stud. Surf. Sci. Catal.* **2002**, *143*, 585. (e) Riahi, G.; Guillemot, D.; Polisset-Thfoin, M.; Khodadadi, A. A.; Fraissard, J. *Catal. Today* **2002**, *72*, 115. (f) Guillon, E.; Lynch, J.; Uzio, D.; Didillon, B. *Catal. Today.* **2001**, *65*, 201. (g) Chan, P. P. Y.; Vanidjee, K.; Adesina, A. A.; Rogers, P. L. *Catal. Today* **2000**, *63*, 379. (h) Humblot, F.; Candy, J. P.; Le Peltier, F.; Didillon, B.; Basset, J. M. *J. Catal.* **1998**, *179* (2), 459. (i) Ugo, R.; Dossi, C.; Psaro, R. *J. Mol. Catal. A: Chem.* **1996**, *107*, 13.

(3) (a) Gross, A. *Top. Catal.* **2006**, *37* (1), 29. (b) Alexeev, O. S.; Gates, B. C. *Ind. Eng. Chem. Res.* **2003**, *42*, 1571. (c) Huber, C.; Moller, K.; Bein, T. *J. Phys. Chem.* **1994**, *98*, 12067. (d) Bergmeister, J. J.; Hanson, B. E. *Organometallics* **1989**, *8*, 283. (e) Guczi, L.; Beck, A. *Polyhedron* **1988**, *7*, 2387. (f) Bender, R.; Braunstein, P. *J. Chem. Soc., Chem. Commun.* **1983**, 334.

10.1021/ic801912x CCC: $40.75
Published on Web 12/05/2008

the supported complex. To this end, in collaborative studies, we examined the selective hydrogenation of phenol to cyclohexanone[9] and the hydrodechlorination of chlorobenzenes to benzene and cyclohexane.[10] In these cases we employed cyanide bridged lanthanide transition metal complexes ($\{(DMF)_{10}Ln_2[Pd(CN)_4]_3\}_4$ Ln = rare earth) as the catalyst precursors, loaded on silica support, and then reduced to metallic nanoparticles. The catalysts obtained proved to be significantly more active than palladium alone and more active than catalysts produced by separate impregnation of the metals onto the support.[9,10]

Our previous investigations have prompted us to extend our Ln−M studies from rare earths to more economical and practical alkaline earth metals (AEM) in view of the ability of alkaline earths to mimic some of the properties of the rare earths. We have recently shown[11] that the cyanide bridged alkaline earth−Pd catalyst precursors $\{(DMF)_xM(\mu\text{-}CN)_yPd(CN)_{4-y}\}_\infty$ (M = Ba, Sr; $x = 3$ or 4; $y = 3$ or 4) can be converted to catalytic nanoparticles on a silica surface for the hydrodechlorination of chlorobenzenes to benzene and the hydrogenation of benzene to cyclohexane. These bimetallic catalysts were observed to be over an order of magnitude more active than palladium alone in the hydrodechlorination reactions.[12] We report here the syntheses and structures of these catalyst precursor alkaline earth−transition metal heterobimetallic complexes $\{(DMF)_xM(\mu\text{-}CN)_yM^*(CN)_{4-y}\}_\infty$ [M = Ba: M* = Ni **1**, M* = Pd **2**, M* = Pt **3**; M = Sr: M* = Ni **4**, M* = Pd **5**, M* = Pt **6**; $x = 3$ or 4, $y = 3$ or 4].

Experimental Section

General Data. All manipulations were carried out on a standard high vacuum line or in a drybox under an atmosphere of dry, pure N_2. DMF (Mallinckrodt) was stirred over pretreated 4 Å molecular sieves for 4−5 days in a Pyrex flask, then was degassed under vacuum, and the flask was connected to a U-tube apparatus in the drybox. The DMF was degassed a second time under vacuum and then distilled at 70−80 °C into a 1000 mL Pyrex flask at −78 °C. The DMF was warmed to room temperature and then stored in the drybox. Linde brand molecular sieves (4 Å) were heated to 150 °C under dynamic vacuum for 24 h prior to use. $K_2[Ni(CN)_4]\cdot H_2O$ (Strem), $K_2[Pd(CN)_4]\cdot 3H_2O$ (Aldrich), and $K_2[Pt(CN)_4]$ (Strem) were all dried under vacuum at 200 °C for 16 h and stored in the drybox. KCN (Strem), $NiCl_2$ (Strem), $PdCl_2$ (Aldrich), $PtCl_2$ (Strem), $BaCl_2$ (Strem), and $SrCl_2$ (Strem) were used as received.

Preparation of $\{(DMF)_xM(\mu\text{-}CN)_yM^*(CN)_{4-y}\}_\infty$ [M = Ba: M* = Ni 1, M* = Pd 2, M* = Pt 3; M = Sr: M* = Ni 4, M* = Pd 5, M* = Pt 6; $x = 3$, or 4; $y = 3$ or 4]. Method 1. The preparations of $\{(DMF)_xM(\mu\text{-}CN)_yM^*(CN)_{4-y}\}_\infty$ [M = Ba, Sr; M* = Ni, Pd, and Pt] are similar. In a typical synthetic procedure, a 1:1 ratio of starting materials, MCl_2 (M = Ba, Sr) (0.5 mmol) and $K_2[M^*(CN)_4]$ (M* = Ni, Pd, and Pt) (0.5 mmol) were charged into a 50 mL reaction flask in the glovebox, and 10 mL of DMF were added to the flask. The mixture was stirred at room temperature over 1 week. The resulting cloudy solution was filtered, removing a white precipitate (KCl). DMF was pumped away (via dynamic vacuum) until a viscous oil remained. Light yellow X-ray quality crystals of **1** and **4** and white X-ray quality crystals of **2**, **3**, **5**, and **6** were formed from DMF solution after 24 h at room temperature: yield: ∼85%. The crystals were dried under dynamic vacuum for 12−14 h. The iso-structural one-dimensional (1D) ladder compounds (**1**, **4**, **5**, and **6**) all lost one DMF molecule per empirical unit, as determined by elemental analysis because of this drying process. The iso-structural two-dimensional (2D) sheet compounds (**2** and **3**) were unaffected by drying, as determined by elemental analysis. $\{(DMF)_4Ba(\mu\text{-}CN)_3Ni(CN)\}_\infty$ (**1**): IR (Nujol mull; ν_{CN}, cm^{-1}): 2120 (m), 2131 (s), 2142 (s). Anal. Calcd for $C_{13}H_{21}N_7O_3BaNi$: C, 30.06, H, 4.08, N, 18.88. Found: C, 30.51, H, 4.39, N, 19.02. $\{(DMF)_3Ba(\mu\text{-}CN)_4Pd\}_\infty$ (**2**): IR (Nujol mull; ν_{CN}, cm^{-1}): 2142 (s). Anal. Calcd for $C_{13}H_{21}N_7O_3BaPd$: C, 27.57, H, 3.73, N, 17.29. Found: C, 27.36, H, 3.56, N, 17.18. $\{(DMF)_3Ba(\mu\text{-}CN)_4Pt\}_\infty$ (**3**): IR (Nujol mull; ν_{CN}, cm^{-1}): 2138 (s). Anal. Calcd for $C_{13}H_{21}N_7O_3BaPt$: C, 23.81, H, 3.23, N, 14.95. Found: C, 24.08, H, 3.49, N, 15.36. $\{(DMF)_4Sr(\mu\text{-}CN)_3Ni(CN)\}_\infty$ (**4**): IR (Nujol mull; ν_{CN}, cm^{-1}): 2119 (m), 2141 (s). Anal. Calcd for $C_{13}H_{21}N_7O_3SrNi$: C, 33.25, H, 4.51, N, 20.88. Found: C, 33.18, H, 4.26, N, 20.66. $\{(DMF)_4Sr(\mu\text{-}CN)_3Pd(CN)\}_\infty$ (**5**): IR (Nujol mull; ν_{CN}, cm^{-1}): 2132 (s), 2153 (vw). Anal. Calcd for $C_{13}H_{21}N_7O_3SrPd$: C, 30.18, H, 4.09, N, 18.95. Found: C, 30.46, H, 4.39, N, 19.28. $\{(DMF)_4Sr(\mu\text{-}CN)_3Pt(CN)\}_\infty$ (**6**): IR (Nujol mull; ν_{CN}, cm^{-1}): 2131 (s), 2143 (s), Anal. Calcd for $C_{13}H_{21}N_7O_3SrPt$: C, 25.76, H, 3.49, N, 16.18. Found: C, 25.99, H, 3.78, N, 16.36.

Method 2. In a typical synthetic procedure a 50 mL reaction flask in a glovebox (N_2) was charged with a 1:1:4 ratio of starting

(4) (a) Dimitratos, N.; Villa, A.; Wang, D.; Porta, F.; Su, D.; Prati, L. *J. Catal.* **2006**, *244*, 113. (b) Ekou, T.; Vicente, A.; Lafaye, G.; Especel, C.; Marecot, P. *Appl. Catal., A: Gen.* **2006**, *314*, 64. (c) Lapisardi, G.; Urfels, L.; Gelin, P.; Primet, M.; Kaddouri, A.; Garbowski, E.; Toppi, S.; Tena, E. *Catal. Today* **2006**, *117*, 564. (d) Moronta, A.; Troconis, M. E.; Gonzalez, E.; Moran, C.; Sanchez, J.; Gonzalez, A.; Quinonez, J. *Appl. Catal., A: Gen.* **2006**, *310*, 199. (e) Serrano-Ruiz, J. C.; Huber, G. W.; Sanchez-Castillo, M. A.; Dumesic, J. A.; Rodriguez-Reinoso, F.; Sepulveda-Escribano, A. *J. Catal.* **2006**, *241*, 378. (f) Boutzeloit, M.; Benitez, V. M.; Mazzieri, V. A.; Especel, C.; Epron, F.; Vera, C. R.; Pieck, C. L.; Marecot, P. *Catal. Commun.* **2006**, *7*, 627. (g) Pawelec, B.; La Parola, V.; Thomas, S.; Fierro, J. L. G. *J. Mol. Catal. A: Chem.* **2006**, *253*, 30. (h) Araya, P.; Ferrada, C.; Cortes, J. *Catal. Lett.* **1995**, *35*, 175. (i) Meriaudeau, P.; Naccache, C.; Thangaraj, A.; Bianchi, C. L.; Carli, R.; Vishvanathan, V.; Narayanan, S. *J. Catal.* **1995**, *154*, 345. (j) Toyir, J.; Leconte, M.; Niccolai, G. P.; Candy, J.; Basset, J.-M. *J. Mol. Catal. A: Chem.* **1995**, *100*, 61. (k) Kovalchuk, V. I.; Kuznetsov, B. N. *J. Mol. Catal. A: Chem.* **1995**, *102*, 103. (l) Ali, J. K.; Rippin, D. W. T. *Ind. Eng. Chem. Res.* **1995**, *34*, 722. (m) Bischoff, S.; Weigt, A.; Fujimoto, K.; Luecke, B. *J. Mol. Catal. A: Chem.* **1995**, *95*, 259.

(5) (a) Silva, A. M.; Santos, O. A. A.; Morales, M. A.; Baggio-Saitovitch, E. M.; Jordao, E.; Fraga, M. A. *J. Mol. Catal. A: Chem.* **2006**, *253*, 62. (b) Barbaro, P.; Bianchini, C.; Dal S, V.; Meli, A.; Moneti, S.; Psaro, R.; Scaffidi, A.; Sordelli, L.; Vizza, F *J. Am. Chem. Soc.* **2006**, *128*, 7065. (c) Borgna, A.; Anderson, B. G.; Saib, A. M.; Bluhm, H.; Haevecker, M.; Knop-Gericke, A.; Kuiper, A. E. T.; Tamminga, Y.; Niemantsverdriet, J. W. *J. Phys. Chem. B* **2004**, *108*, 17905.

(6) (a) Lambert, S.; Ferauche, F.; Brasseur, A.; Pirard, J.-P.; Heinrichs, B. *Catal. Today* **2005**, *100*, 283. (b) Nutt, M. O.; Hughes, J. B.; Wong, M. S. *Environ. Sci. Technol.* **2005**, *39*, 1346. (c) Simagina, V.; Likholobov, V.; Bergeret, G.; Gimenez, M. T.; Renouprez, A. *Appl. Catal. B: Environ.* **2003**, *40*, 293.

(7) Llorca, J.; Homs, N.; Rossell, O.; Seco, M.; Fierro, J.-L. G.; Ramirez de la Piscina, P. *J. Mol. Catal. A: Chem.* **1999**, *149*, 225.

(8) Rath, A.; Liu, J.; Shore, S. G.; Aceves, E.; Mitome, J.; Ozkan, U. S. *J. Mol. Catal. A: Chem.* **2001**, *165*, 103.

(9) (a) Shore, S. G.; Ding, E.; Park, C.; Keane, M. A. *J. Mol. Catal. A: Chem.* **2004**, *212*, 291. (b) Shore, S. G.; Ding, E.; Park, C.; Keane, M. A. *Catal. Commun.* **2002**, *3*, 77.

(10) (a) Jujjuri, S.; Ding, E.; Hommel, E. L.; Shore, S. G.; Keane, M. A. *J. Catal.* **2006**, *239*, 486. (b) Jujjuri, S.; Ding, E.; Shore, S. G.; Keane, M. A. *Appl. Organomet. Chem.* **2003**, *17*, 493.

(11) Ding, E.; Jujjuri, S.; Sturgeon, M.; Shore, S. G.; Keane, M. A. *J. Mol. Catal. A: Chemical* **2008**, *294*, 51.

(12) Shore, S. G.; Ding, E.; Keane, M. A. Patent Application, International Patent App. No. PCT/US08/77448.

materials, MCl_2 (M = Ba, Sr) (0.5 mmol), M*Cl_2 (M* = Ni, Pd, and Pt) (0.5 mmol) and KCN (2.0 mmol); 15 mL of DMF were added to the flask. The mixture was stirred at room temperature over 2 weeks. The resulting mixture was filtered to remove a white precipitate (KCl). DMF was removed (via dynamic vacuum) until a viscous oil remained. X-ray quality crystals, which confirm the synthesis of complexes **1**−**6**, were formed after 24 h at room temperature: yield: ∼80%.

X-ray Structure Determination. Single crystal X-ray diffraction data were collected using graphite monochromated Mo Kα radiation (λ = 0.71073 Å) on an Enraf-Nonius Kappa CCD diffraction system. Single crystals of **1**−**6** were mounted on the tip of a glass fiber coated with Fomblin (a pentafluoropolyether) oil, and crystallographic data were collected at 150 K. Unit cell parameters were obtained by indexing the peaks from the first 10 frames and refined employing the whole data set. All frames were integrated and corrected for Lorentz and polarization effects using Denzo-SMN package (Nonius BV, 1999).[13] An absorption correction was applied using the SORTAV program[14] provided by MaXus software.[15] The structure was solved by direct methods and refined using the SHELXTL-97[16] (difference electron density calculation, full matrix least-squares refinements). All non-hydrogen atoms were located and refined anisotropically, hydrogen atom positions were calculated assuming standard geometries.

Catalyst Preparation. Ba−Pd/SiO_2 and Sr−Pd/SiO_2 samples were prepared by contacting SiO_2 (fumed, Sigma-Aldrich) with a solution of the bimetallic precursor (**2** and **5**, respectively) in DMF to deliver a 5% w/w Pd loading. The DMF was removed from the metal impregnated SiO_2 via dynamic vacuum over a period of 12 h at room temperature. IR spectra of the samples confirm that the structures of bimetallic complexes were retained upon impregnation. Figure 1a and 1b show the CN stretching frequencies of **2** and **5**, respectively; full spectra are available in the Supporting Information.

For comparison purposes, a monometallic 5% w/w Pd/SiO_2 was prepared by contacting the same SiO_2 substrate with a DMF solution of palladium acetate. Prior to catalysis, the samples were activated in a fixed bed tubular glass reactor (i.d. = 1.25 cm) by heating (10 K min^{-1}) in a 60 cm^3 min^{-1} stream of dry ultrapure H_2 to a final temperature of 573 K that was maintained for 12 h. Catalytic activity was tested in a plug flow catalytic reactor operated under isothermal conditions. Full details of the catalytic procedure and results are available elsewhere.[11]

Results and Discussion

Synthesis and Characterization of $\{(DMF)_xM(\mu\text{-}CN)_y\text{-}M^*(CN)_{4-y}\}_\infty$ [M = Ba: M* = Ni 1, M* = Pd 2, M* = Pt 3; M = Sr: M* = Ni 4, M* = Pd 5, M* = Pt 6; *x* = 3 or 4; *y* = 3 or 4]. The preparative procedure to obtain complexes **1**−**6** was the same throughout; all of which can be produced from MCl_2 and $K_2[M^*(CN)_4]$ (eq 1) or from MCl_2, M*Cl_2 and KCN (eq 2) in DMF via metathesis reactions in high yield. The rather lengthy reaction time (1 to 2 weeks) was due to the poor solubility of MCl_2 in DMF. After the reaction was complete and KCl removed, high quality single crystals were formed from concentrated DMF solution.

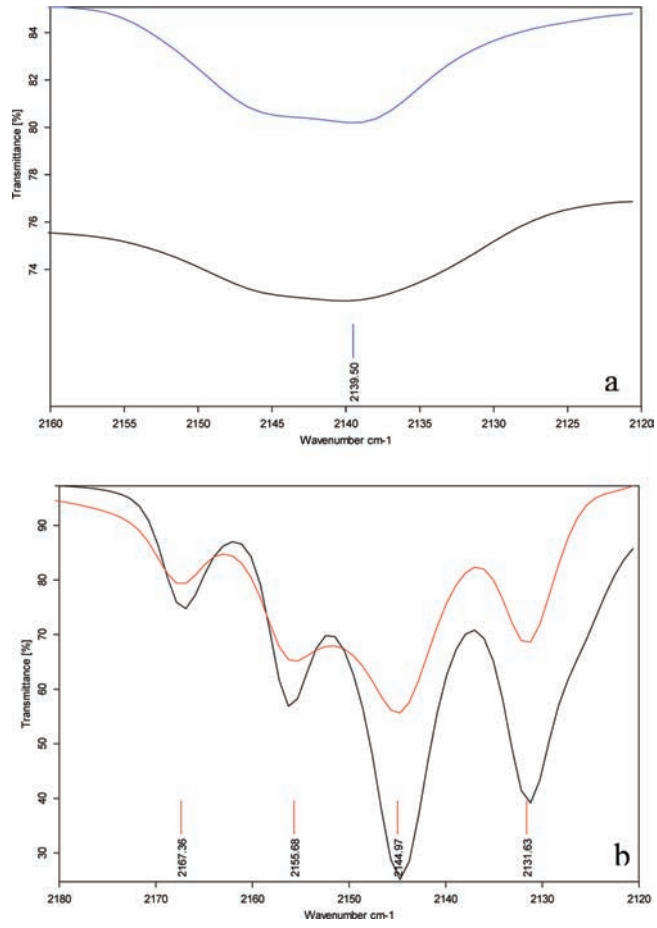

Figure 1. CN stretching frequency in the IR spectra of **2** (a) and **5** (b) loaded onto a SiO_2 support; in both a and b the upper (colored) spectra are KBr presses of the crystalline materials and the lower (black) spectra are Nujol mulls of the material loaded onto SiO_2 support.

$$MCl_2 + K_2[M^*(CN)_4] \xrightarrow{DMF} \{(DMF)_xM(\mu\text{-}CN)_yM^*(CN)_{4-y}\}_\infty + 2KCl \quad (1)$$

M = Ba and Sr; M* = Ni, Pd, and Pt; *x* = 3 or 4, *y* = 3 or 4

$$MCl_2 + M^*Cl_2 + 4KCN \xrightarrow{DMF} \{(DMF)_xM(\mu\text{-}CN)_yM^*(CN)_{4-y}\}_\infty + 4KCl \quad (2)$$

M = Ba and Sr; M* = Ni, Pd, and Pt; *n* = 3 or 4

The light yellow (**1** and **4**) or white (**2**, **3**, **5**, and **6**) solids of complexes **1**−**6** are very stable at room temperature in the absence of air, either in the solid state or in a DMF solution.

X-ray Structural Results of 1−6. The solid state structures of $\{(DMF)_4Ba(\mu\text{-}CN)_3Ni(CN)\}_\infty$ **1**, $\{(DMF)_3Ba(\mu\text{-}CN)_4Pd\}_\infty$ **2**, $\{(DMF)_3Ba(\mu\text{-}CN)_4Pt\}_\infty$ **3**, $\{(DMF)_4Sr(\mu\text{-}CN)_3Ni(CN)\}_\infty$ **4**, $\{(DMF)_4Sr(\mu\text{-}CN)_3Pd(CN)\}_\infty$ **5**, and $\{(DMF)_4Sr(\mu$-

(13) Otwinowski, Z.; Minor, W. In *Methods in Enzymology.*; Carter, C. W., Jr., Sweet, R. M., Eds.; Academic Press: New York, 1997; Vol. *276(A)*, p 307.
(14) (a) Blessing, R. H. *Acta Crystallogr., Sect. A* **1995**, *51*, 33. (b) Blessing, R. H. *J. Appl. Crystallogr.* **1997**, *30*, 421.
(15) Mackay, S.; Gilmore, C. J.; Edwards, C.; Tremayne, M.; Stuart, N.; Shankland, K. *MaXus: A computer program for the solution and refinement of crystal structures from diffraction data*; University of Glasgow, Nonius BV, and Mac- Science Co. Ltd., Scotland, U.K.; Delft, The Netherlands; and Yokohama, Japan, 1998.
(16) *SHELXTL*, version 5.10; Bruker Analytical X-ray systems: Madison, WI, 1997.

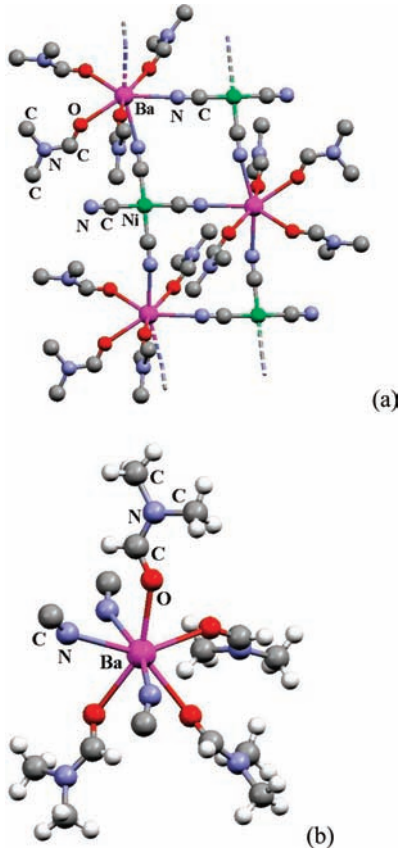

Figure 2. Molecular structure of a portion of the 1D array (a) and coordination geometry about alkaline earth center (b) in complex $\{(DMF)_4Ba(\mu\text{-}CN)_3Ni(CN)\}_\infty$ **1**. Complexes $\{(DMF)_4Sr(\mu\text{-}CN)_3Ni(CN)\}_\infty$ **4**, $\{(DMF)_4Sr(\mu\text{-}CN)_3Pd(CN)\}_\infty$ **5**, and $\{(DMF)_4Sr(\mu\text{-}CN)_3Pt(CN)\}_\infty$ **6** are isostructural with **1**.

$CN)_3Pt(CN)\}_\infty$ **6** were determined by a single-crystal X-ray diffraction analyses. Structures of **1**, **4**, **5**, and **6** are shown in Figure 2 and structures **2** and **3** are shown in Figure 3. Crystallographic data are given in Tables 1 and 2. Selected bond distances were averaged and are tabulated in Table 3.

Single-crystal X-ray diffraction analysis show that complexes **1**, **4**, **5**, and **6** form isostructural 1D "ladder" arrays through isocyanide linkages (Figure 2). These complexes are also isostructural with the cyanide-bridged divalent lanthanide-transition metal complexes $[\{(DMF)_4EuM(CN)_4\}_\infty$ M = Ni, or Pt] that we reported earlier.[17]

In these complexes, the alkaline earth ions are coordinated to four DMF ligands through the oxygen atoms and are also coordinated to three bridging cyanide ligands through the nitrogen atoms (Figure 2b). The Ba−N distances in complex **1** range from 2.819(3) Å to 2.846(3) Å, while the Sr−N distances are in the range from 2.643(4) Å to 2.674(4) Å **4**, 2.637(3) Å to 2.680(3) Å **5**, and 2.644(4) Å to 2.677(4) Å **6**. The TM−C (TM = Ni **1**, Ni **4**, Pd **5**, Pt **6**) bond lengths vary somewhat within each structure: 1.859(4) Å to 1.872(4) Å **1**, 1.863(5) Å to 1.876(5) Å **4**, 1.988(4) Å to 2.003(4) Å **5**, and 1.988(5) Å to 2.001(5) Å **6.** The C≡N bond distances in **1** and **4** do not vary outside of the estimated errors: 1.150(5) Å to 1.156(5) Å **1** and 1.148(6) Å to 1.156(6) Å **4**. However, in **5** and **6** there is some variance in the C≡N bond distances. In **5** the longest C≡N distance (1.151(5) Å) is trans to the shortest C≡N distance (1.136(5) Å), they are

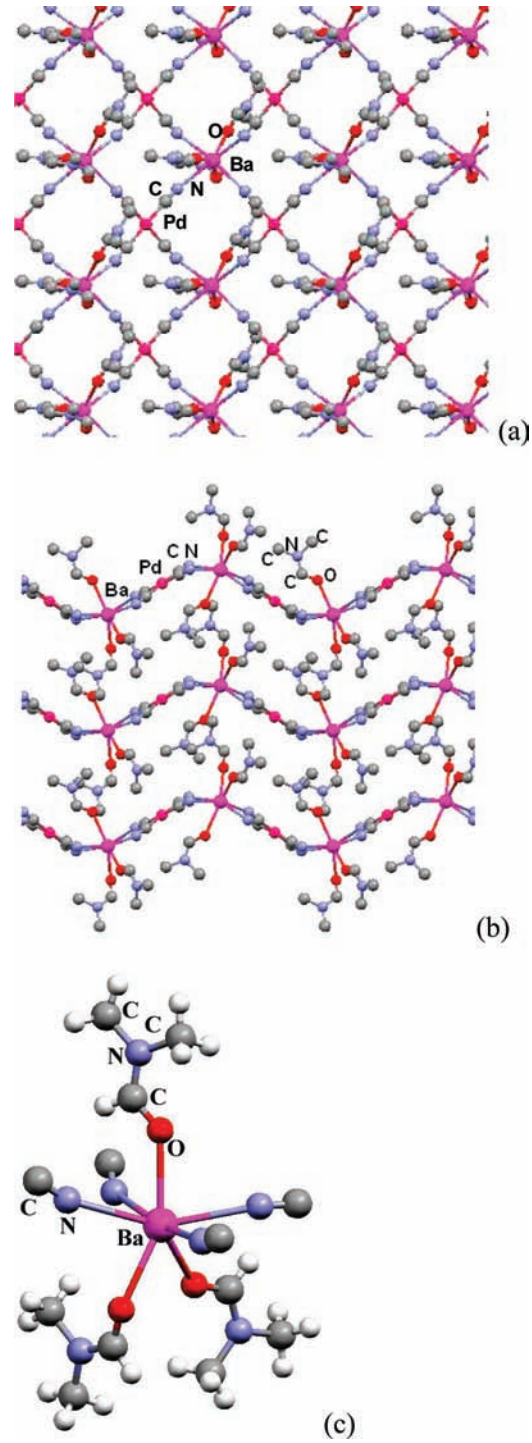

Figure 3. Molecular structures of a 2D puckered sheet array of complex $\{(DMF)_3Ba(\mu\text{-}CN)_4Pd\}_\infty$ **2** (a, b) and Coordination geometries about Ba center in **2** (c). $\{(DMF)_3Ba(\mu\text{-}CN)_4Pt\}_\infty$ **3** is isostructural with **2**.

both bridging cyanides (Figure 2). The terminal cyanide in **6** has the shortest C≡N distance (1.135(5) Å). The longest C≡N distance (1.155(7) Å) is a bridging cyanide cis to the shortest C≡N distance. The geometries around the nickel, palladium, and platinum atoms are slightly distorted square planar configurations.

Unlike the 1D extended array structures of complexes **1**, **4**, **5**, and **6**, complexes $\{(DMF)_3Ba(\mu\text{-}CN)_4Pd\}_\infty$ **2** and $\{(DMF)_3Ba(\mu\text{-}CN)_4Pt\}_\infty$ **3** crystallize as isostructural 2D puckered layer structures, Figure 3.

Table 1. Crystallographic Data for $\{(DMF)_4Ba(\mu\text{-}CN)_3Ni(CN)\}_\infty$ **1**, $\{(DMF)_4Sr(\mu\text{-}CN)_3Ni(CN)\}_\infty$ **4**, $\{(DMF)_4Sr(\mu\text{-}CN)_3Pd(CN)\}_\infty$ **5**, and $\{(DMF)_4Sr(\mu\text{-}CN)_3Pt(CN)\}_\infty$ **6**

empirical formula	$C_{16}H_{28}N_8O_4BaNi$	$C_{16}H_{28}N_8O_4SrNi$	$C_{16}H_{28}N_8O_4SrPd$	$C_{16}H_{28}N_8O_4SrPt$
fw (amu)	592.52	542.79	590.48	679.17
cryst syst	triclinic	triclinic	triclinic	triclinic
space group	$P\bar{1}$	$P\bar{1}$	$P\bar{1}$	$P\bar{1}$
a, Å	8.935(2)	8.875(1)	8.924(2)	8.8921(2)
b, Å	11.175 (3)	10.954(3)	11.162(3)	11.160(2)
c, Å	12.539(3)	12.392(3)	12.519(3)	12.438(3)
α, deg	82.08(3)	83.09(3)	82.98(3)	83.24(3)
β, deg	86.06(3)	86.79(3)	86.81(3)	86.87(3)
γ, deg	86.06(3)	84.82(3)	84.01(3)	83.85(3)
V, Å^3	1234.8(2)	1189.9(2)	1229.7(2)	1217.6(5)
Z	2	2	2	2
ρ (calcd), g cm^{-3}	1.594	1.515	1.595	1.853
T, *K*	150(2) K	150(2)	173(2)	150(2)
absorption coefficient (mm^{-1})	2.382	3.069	2.935	7.965
final *R* indices [$I > 2\sigma(I)$ data][a,b]	$R_1 = 0.0261$, $wR_2 = 0.0701$	$R_1 = 0.0445$, $wR_2 = 0.1153$	$R_1 = 0.0314$, $wR_2 = 0.0814$	$R_1 = 0.0321$, $R_2 = 0.0801$
R indices (all data)	$R_1 = 0.0319$, wR2 = 0.0723	$R_1 = 0.0644$, $wR_2 = 0.1246$	$R_1 = 0.0373$, $wR_2 = 0.0846$	$R_1 = 0.0364$, $wR_2 = 0.0822$

[a] $R_1 = \sum||F_o| - |F_c||/\sum|F_o|$. [b] $wR_2 = \{\sum[w(F_o^2 - F_c^2)^2]/\sum w(F_o^2)^2\}^{1/2}$.

Table 2. Crystallographic Data for $\{(DMF)_3Ba(\mu\text{-}CN)_4Pd\}_\infty$ **2** and $\{(DMF)_3Ba(\mu\text{-}CN)_4Pt\}_\infty$ **3**

empirical formula	$C_{13}H_{21}N_7O_3BaPd$	$C_{13}H_{21}N_7O_3BaPt$
fw (amu)	567.11	655.80
cryst syst	monoclinic	monoclinic
space group	*Cc*	*Cc*
a, Å	7.892(2)	7.8934(16)
b, Å	16.542(3)	16.530(3)
c, Å	16.083(3)	16.085(3)
α, deg	90.00	90.00
β, deg	90.48(3)	90.38(3)
γ, deg	90.00	90.00
V, Å^3	2099.4(3)	2098.7(7)
Z	4	4
ρ (calcd), g cm^{-3}	1.794	2.076
T, *K*	150(2)	150(2)
absorption coefficient (mm^{-1})	2.745	8.548
final *R* indices [$I > 2\sigma(I)$ data][a,b]	$R_1 = 0.0270$, $wR_2 = 0.0687$	$R_1 = 0.0332$, $wR_2 = 0.0694$
R indices (all data)	$R_1 = 0.0279$, $wR_2 = 0.0689$	$R_1 = 0.0385$, $wR_2 = 0.0714$

[a] $R_1 = \sum||F_o| - |F_c||/\sum|F_o|$. [b] $wR_2 = \{\sum[w(F_o^2 - F_c^2)^2]/\sum w(F_o^2)^2\}^{1/2}$.

Table 3. Selected Average Bond Distances (Δ) for **1**−**6**[a]

	1	**2**	**3**	**4**	**5**	**6**
M−O	2.687(3)	2.675(4)	2.688(7)	2.534(3)	2.528(3)	2.529(3)
M−N	2.833(3)	2.860(5)	2.854(9)	2.661(4)	2.658(3)	2.660(4)
C−N	1.154(5)	1.144(7)	1.150(12)	1.151(6)	1.144(5)	1.146(6)
M*−C	1.867(4)	1.998(5)	1.994(9)	1.870(5)	1.995(4)	1.996(5)

[a] M = Alkaline Earth; M* = Transition Metal.

Similar 2D structures have not been observed in the cyanide-bridged lanthanide-transition metal complexes that we reported previously.[17,18] The barium atoms in **2** and **3** are seven-coordinated (Figure 3) as in complex **1**. However, in the 2D sheet arrays, the barium is coordinated to four bridging cyanide ligands (instead of three, as in **1**) and only three DMF ligands (instead of four, as seen in **1**). The four Ba−N bond distances vary between 2.846(4) Å to 2.889(5) Å in **2** and 2.840(8) Å to 2.868(8) Å in **3**. The Ba−N bond distances in **2** and **3** are slightly longer than in **1**. The palladium atoms in **2** and platinum atoms in **3** are covalently bonded to four CN^- ligands in an approximately square planar geometry with almost linear Pd−C−N angles. In **2**, the Pd−C distances (1.991(5) Å, 1.999(5) Å, 2.000(5) Å, and 2.002(5) Å) are all similar; as are the C≡N distances (1.147(7) Å, 1.144(7) Å, 1.143(7) Å, and 1.143(7) Å). In **3**, the Pt−C distances are similar (1.970(9) Å, 1.981(9) Å, 2.009(9) Å, and 2.010(9) Å); however, only the two cis C≡N distances are similar (1.33(1) Å and 1.139(1) Å, 1.162(1) Å and 1.164(1) Å). Here one should expect all four C≡N distances to be similar because of the symmetric environment of the cyanide ligands.

From Figures 2 and 3 the observed coordination environments of barium in the 1D ladder and 2D sheet structures are very similar. Exchanging a DMF ligand for a bridging CN^- is the key to producing the 2D sheet. It is currently unclear as to why $\{(DMF)_4Ba(\mu\text{-}CN)_3Ni(CN)\}_\infty$ **1** crystallizes as the 1D ladder and not the 2D sheet, as seen in the other Ba containing complexes **2** and **3**. It is of interest to note that a similar two structure phenomenon exists in the Ln−Ni bimetallic compounds previously studied,[17,18] where there is a kinetically favored single strand chain structure and a thermodynamically stable double stranded chain structure. Depending on crystallization conditions, either structure is obtainable.

Infrared Spectra. Similar absorption bands are observed in the solid state infrared spectral patterns for complexes **1**, **4**, **5**, and **6**. Multiple bands in the CN stretching region are present because of the different environments of the cyanide (i.e., terminal and bridging). It should also be noted that there are two types of bridging cyanide ligands in compounds **1**, **4**, **5**, and **6** (cis and trans); these different bridging environments give rise to different stretching modes. The lowest

(17) Knoeppel, D. W.; Shore, S. G. *Inorg. Chem.* **1996**, *35*, 5328.

(18) (a) Liu, S.; Poplaukhin, P.; Ding, E.; Chen, X.; Keane, M. A.; Shore, S. G. *J. Alloys. Compd.* **2006**, *418*, 21. (b) Plecnik, C.; Liu, S.; Shore, S. G. *Acc. Chem. Res.* **2003**, *36*, 499. (c) Liu, J.; Knoeppel, D. W.; Liu, S.; Meyers, E. A.; Shore, S. G. *Inorg. Chem.* **2001**, *40*, 2842. (d) Du, B.; Ding, E; Meyers, E. A.; Shore, S. G. *Inorg. Chem.* **2001**, *40*, 3637. (e) Du, B.; Meyers, E. A.; Shore, S. G. *Inorg. Chem.* **2000**, *39*, 4639. (f) Liu, J.; Meyers, E. A.; Shore, S. G. *Inorg. Chem.* **1998**, *37*, 5410. (g) Knoeppel, D. W.; Liu, J.; Meyers, E. A.; Shore, S. G. *Inorg. Chem.* **1998**, *37*, 4828. (h) Liu, J.; Meyers, E. A.; Cowan, J. A.; Shore, S. G. *Chem. Commun.* **1998**, 2043. (i) Shore, S. G.; Deng, H.; Knoeppel, D. W.; Liu, J.; White, J. P., III; Chun, S.-H. *J. Alloys Compd.* **1997**, *249*, 25. (j) Knoeppel, D. W.; Shore, S. G. *Inorg. Chem.* **1996**, *35*, 1747. (k) Deng, H.; Chun, S. H.; Florian, P.; Grandinetti, P. J.; Shore, S. G. *Inorg. Chem.* **1996**, *35*, 3891. (l) Knoeppel, D. W.; Shore, S. G. *Inorg. Chem.* **1996**, *35*, 5328.

wave numbers for **1** (2120 cm^{-1}), **4** (2119 cm^{-1}), **5** (2132 cm^{-1}), and **6** (2131 cm^{-1}) are assigned to the terminal cyanide stretching frequency, while the higher wave numbers for **1** (2142 cm^{-1}), **4** (2141 cm^{-1}), **5** (2153 cm^{-1}), and **6** (2143 cm^{-1}) are assigned to the bridging cyanide stretching frequency.

The infrared spectral patterns for complexes **2** and **3** are distinctly different from those observed in complexes **1**, **4**, **5**, and **6**, showing only one absorption band at 2142 cm^{-1} **2** and 2138 cm^{-1} **3**. Only one band due to CN stretching is expected, as all the cyanides in this 2D structure are bridging. Single-crystal X-ray diffraction analysis for **2** and **3** confirmed that only bridging cyanides are present (Figure 3).

Application of Alkaline Earth−Transition Metal Bimetallic in Heterogeneous Catalysis. Taking the 2D array structure (Pd−Ba) and ladder structure (Pd−Sr) bimetallic combinations as representative cases, the catalytic activity of the silica supported bimetallics in chlorobenzene hydrodechlorination have been assessed against that of silica supported Pd. Time on-stream conversion and reaction selectivity data are presented and subjected to a detailed analysis elsewhere.[11] Both bimetallic catalysts delivered specific dechlorination rates (normalized per unit Pd surface area) that were over an order of magnitude greater than that achieved with Pd/SiO_2, as can be seen from the data given in Table 4. The higher reaction rates delivered by the bimetallics suggest a surface synergy resulting in enhanced hydrogenolysis activity. These results demonstrate that our alkaline earth−transition metal complexes can serve as precursors for the synthesis of supported bimetallic catalysts, which exhibit appreciably greater hydrogenolysis activities when compared with a conventional supported Pd catalyst. This success has encouraged us to continue our ventures in converting our cyanide bridged extended arrays into supported bimetallic catalysts.

Table 4. Specific Hydrodechlorination Rates Recorded for Pd/SiO_2, $Ba-Pd/SiO_2$ and $Sr-Pd/SiO_2$ in the Conversion of Chlorobenzene and 1,2-Dichlorobenzene

	R (mol_{Cl} h^{-1} m^{-2})	
catalyst	chlorobenzene	1,2-dichlorobenzene
Pd/SiO_2	0.24	0.04
$Sr-Pd/SiO_2$	0.58	0.57
$Ba-Pd/SiO_2$	0.85	0.78

Acknowledgment. This work was supported by the National Science Foundation through Grants CHE 02-13491 and CTS-0218591.

Supporting Information Available: FT-IR spectra and X-ray crystallographic files for structural analysis of the compounds $\{(DMF)_4BaNi(CN)_4\}_\infty$ **1**, $\{(DMF)_3BaPd(CN)_4\}_\infty$ **2**, $\{(DMF)_3BaPt(CN)_4\}_\infty$ **3**, $\{(DMF)_4SrNi(CN)_4\}_\infty$ **4**, $\{(DMF)_4SrPd(CN)_4\}_\infty$ **5**, and $\{(DMF)_4SrPt(CN)_4\}_\infty$ **6** in CIF format. This material is available free of charge via the Internet at http://pubs.acs.org.

IC801912X